



HAL
open science

Comparison of the tribological properties of carbon/glass fiber reinforced PA66-based composites in contact with steel, with and without grease lubrication

Takeshi Kunishima, Yasuharu Nagai, Gaetan Bouvard, Jean-Christophe Abry, Vincent Fridrici, Philippe Kapsa

► To cite this version:

Takeshi Kunishima, Yasuharu Nagai, Gaetan Bouvard, Jean-Christophe Abry, Vincent Fridrici, et al.. Comparison of the tribological properties of carbon/glass fiber reinforced PA66-based composites in contact with steel, with and without grease lubrication. *Wear*, 2021, 477, 10.1016/j.wear.2021.203899 . hal-04084014

HAL Id: hal-04084014

<https://hal.science/hal-04084014>

Submitted on 22 Jul 2024

HAL is a multi-disciplinary open access archive for the deposit and dissemination of scientific research documents, whether they are published or not. The documents may come from teaching and research institutions in France or abroad, or from public or private research centers.

L'archive ouverte pluridisciplinaire **HAL**, est destinée au dépôt et à la diffusion de documents scientifiques de niveau recherche, publiés ou non, émanant des établissements d'enseignement et de recherche français ou étrangers, des laboratoires publics ou privés.



Distributed under a Creative Commons Attribution - NonCommercial 4.0 International License

Comparison of the tribological properties of carbon/glass fiber reinforced PA66-based composites in contact with steel, with and without grease lubrication

Takeshi Kunishima ^{a, b}, Yasuharu Nagai ^a, Gaëtan Bouvard ^b, Jean-Christophe Abry ^b, Vincent Fridrici ^b, and Philippe Kapsa ^b

^a JTEKT CORPORATION, 333 Toichi-cho, Kashihara, Nara 634-8555, Japan

^b Laboratoire de Tribologie et Dynamique des Systèmes, UMR CNRS 5513, Ecole Centrale de Lyon, Université de Lyon, 36 avenue Guy de Collongue, F-69134 Ecully cedex, France

Corresponding author: Takeshi Kunishima

E-mail: takeshi_kunishima@jtekt.co.jp

Keywords: Polyamide, Carbon fibers, Glass fibers, Grease, Worm gear, Wear, Friction

ABSTRACT

Polyamide 66 (PA66) is used for polymer sliding parts, and to increase its strength, reinforcement fibers such as glass fiber (GF) and carbon fiber (CF) are often added. Using fiber-reinforced composites for sliding parts leads to wear of the composites, which is related to peeled-off fibers and polymer scratching during sliding. Moreover, this has a destructive effect on the steel counterpart. In this work, the tribological properties of grease-lubricated CF-reinforced PA66 were studied and compared to those of GF-reinforced PA66; the effect of CF reinforcement was also studied under dry conditions. The CF composite exhibited poorer tribological properties than those of the GF composite under grease lubrication due to the insufficient interfacial adhesion between the PA66 and fibers, regardless of the PA66 molecular mass, whereas the CF composite exhibited lower friction under dry conditions. Higher wear of the steel counterpart was observed when tested with the CF composite; however, CF is softer than GF, indicating that the destructive effects are not determined by fiber hardness alone. Tribochemistry related to the grease additives on the sliding surface was studied based on the fiber type, ambient temperature, and contact pressure, and tribofilm formation can explain the improvement of the tribological properties.

1. Introduction

Polyamide 66 (PA66) exhibits outstanding mechanical properties including excellent heat resistance and is used for various parts in automobiles and industrial machines such as gears [1–4], bearing retainers [5, 6], and rollers [7]. However, grease lubrication is necessary for severe contact geometries under high contact pressures, such as the meshing of a polymer worm wheel and metallic worm shaft in a worm reducer for automotive electric power steering, to reduce the friction and heat generated by sliding [8–10]. To downsize these parts and use them under severe conditions, PA66 has been reinforced with glass fibers (GFs) and carbon fibers (CFs) to improve its mechanical properties. In the authors' previous study [11], the tribological behavior of GF-reinforced PA66 in contact with steel under grease lubrication was elucidated. The mechanism of wear and creep of the GF-reinforced composite was investigated by observing how the damage on the sliding surface and

mechanical properties of the composite sliding surface changed over time. The wear mechanism of the steel counterpart was discussed considering the quantitative orientation of fibers on the sliding surface of the GF-reinforced composite, and the influence of the hardness of the steel counterpart on the wear of both the composite and steel was elucidated. In another work by the authors [12], the tribochemistry of the grease additives on the sliding surface of a GF-reinforced PA66 composite in contact with steel was investigated. The compositions of the tribofilms on the steel surface and composite surface were chemically analyzed, and the tribofilm formation explained the improvement of the tribological properties as well as their temperature dependence. In addition, the effects of the composition of GF-reinforced PA66 on the tribological properties were investigated [13]. The good interfacial adhesion between the PA66 and GF, an increase in the molecular mass of PA66, and small diameter GFs ensured good wear and creep resistance of the composite, low friction, and good wear resistance of the steel counterpart.

CFs are widely used in various fields, such as automobile and aerospace industries (aircraft and space systems), military, construction, and sporting goods [14]. The cost of CFs is significantly higher than that of GFs [15, 16]; however, CFs exhibit certain advantages over GFs, i.e., excellent tensile properties, low density, high thermal stability, and good thermal and electrical conductivities [14]. Two different types of CFs — PAN (polyacrylonitrile) type and mesophase pitch type — are well known. CFs have also been used for several years to improve the tribological properties of plastics and numerous studies on the tribological properties of CF composites have been conducted. Tewari et al. [17] reported the wear resistance of a CF-reinforced PA66 composite under dry conditions in abrasive wear mode (in contact with SiC abrasive paper) and compared it to the friction and wear properties in the adhesive wear mode. The wear of the CF composite increased as the CF concentration increased in the abrasive wear test, whereas the friction coefficient and wear of the composite decreased as the CF concentration increased in the adhesive wear test. The deterioration of the abrasive wear resistance was attributed to the decrease in the elongation of the composite as the CF concentration increased. Furthermore, the addition of polytetrafluoroethylene (PTFE) to the CF-reinforced PA66 composite increased the abrasive wear of the composite and improved the tribological properties in the adhesive wear mode. Therefore, the effects of the CF addition on the tribological properties are dependent on the wear mode. Zhou et al. [18] found that the wear rate of polyamide 6/polyphenylene sulfide-CF composites in the adhesive wear mode generally increased as the CF concentration increased for sliding tests between a chromium steel ball and CF composite disk. Senthilvelan et al. [19] presented the differences in the failure modes of spur gears made from unreinforced, GF-reinforced, and CF-reinforced PA66; the addition of CFs to the PA66 matrix improved the thermal resistance of the composite. No appreciable tooth shape deformation or molten material layer formation was observed on the fractured surfaces of the CF-reinforced gears, whereas severe plastic deformation at high applied stresses and cracking at the root and tooth surfaces at low stresses were observed in the unreinforced gears. Sharma et al. [20] reported that the enhancement in the interfacial adhesion between polyethersulfone (PES) and CFs by cold remote nitrogen-oxygen plasma treatment improved the mechanical and tribological properties (friction coefficient and wear rate) of the composite.

However, few studies have focused on the tribological properties of a CF-reinforced composite in contact with a metallic material under grease or oil lubrication. Li et al. [21] demonstrated that treating CFs with a rare

earth solution enhanced the wear resistance of CF-reinforced polyimide (PI) in contact with oil-lubricated GCr15 steel by improving the interfacial adhesion between the CFs and PI. Zhao et al. [22] investigated the tribological properties of PI reinforced with various fillers, such as CF, GF, and ZnS particles, in contact with oil-lubricated GCr15 steel with poly-alpha-olefins and found that the reinforcing fibers improved the wear resistance of the composites. The addition of GFs was more effective at improving wear resistance than the addition of CFs, and a synergistic effect between the GFs and ZnS was also observed. Kurokawa et al. [23] reported the performance of lithium grease-lubricated CF-reinforced poly-ether-ether-ketone (PEEK) gears using a pair of CF-reinforced PEEK gears and a CF-reinforced PEEK gear and steel gear combination. The wear resistance of the composite was influenced by CF properties such as the affinity between CFs and PEEK and the strength/modulus of the CFs. However, a detailed explanation of the wear mechanism of the CF-reinforced PA66 composite under grease lubrication was not provided in these studies.

When considering the sliding of a fiber-reinforced composite in contact with a steel counterpart, it is important to consider the destructive effects of the reinforcement fibers on the steel parts; this is because the steel wear related to the destructive effect of the reinforcement fibers in the composite (e.g., the wear of a steel worm shaft in the worm reducer of an electric power steering system) increases the sliding friction and results in insufficient gear durability via the meshing failure of the worm shaft and composite worm wheel. Previously, the authors found that the wear of the steel counterpart can be reduced not only by increasing its hardness but also by adjusting the composition of the composite (such as increasing the molecular mass) using smaller diameter GFs and improving the interfacial adhesion between the GFs and the PA66 [13]. The Mohs hardness of CF (0.5 – 2) is lower than that of GF (6 – 6.5) [24], and CFs are considered to be less destructive to the steel counterpart than GFs. Theberge et al. [25] focused on the differences in the abrasive effects of CFs and GFs and found that polymers reinforced with GFs caused at least ten times as much wear on a relatively soft counter-face, such as mild steel, than polymers reinforced with CFs. Lancaster [26] reported that GF-reinforced PA66 and PTFE cause appreciably more wear and damage to steel than those reinforced with CFs. In addition, the wear rate of a counterpart bronze ball tested with 30 % GF-reinforced PA66 was 36.5 times greater than that tested with a 30 % CF-reinforced polymer. However, there are few works on the effect of the counterpart steel or the composition of the CF composite on the tribological properties of a CF composite in contact with steel under grease lubrication.

This work focused on clarifying the tribological mechanism of CF-reinforced PA66 composites in contact with a steel counterpart under grease lubrication. The differences in the tribological properties of the CF composite under dry and grease lubrication were investigated. The effects of the molecular mass of PA66, hardness of the counterpart steel, and temperature on the tribological properties (wear and creep resistance of the composite and counterpart steel wear resistance) were studied under grease lubrication conditions, and the properties of unreinforced, CF-reinforced, and GF-reinforced PA66 were compared.

2. Experimental

2.1 PA66 and reinforcement fibers

CF-reinforced PA66 test specimens composed of PA66 with various molecular masses were fabricated via

injection molding with commercially available pellets using a ROBOSHOT S-2000i 100B (FANUC Corporation). The viscosity numbers (VNs) of the specimens, which are correlated with the PA66 molecular mass, were measured via the relative viscosity method, according to the ISO307 standard, with a formic acid solvent at 25 °C. The composition and mechanical properties of each evaluated material are listed in Table 1. For comparison, a GF-reinforced PA66 composite and commercially available unreinforced PA66 were also evaluated; the detailed fabrication process of the GF composite is presented in the authors' previous study [11, 12, 13]. The volume fractions of the fibers in the GF 15 % composite and CF 10 % composite (in wt.%) were similar because of the difference in the density of the fibers, as listed in Table 1. In addition, Young's modulus of the CF 10 % composite was higher than that of the GF 15 % composite. Therefore, the GF 33 % composite, which had a similar Young's modulus to the CF 10 % composite, was also prepared to investigate the effects of the contact pressure on the tribological properties.

Table 1 Composition and properties of the test specimens.

Sample no.	Polymer	Fiber type	Fiber fraction (wt.%)	Fiber fraction (vol.%)	VN (ml/g)	Density (g/cm ³)	Tensile Young's modulus at room temperature (GPa)
No. 1	Normal PA66	CF	10	6.8	150	1.18	9.5 ± 0.6
No. 2	High molecular mass PA66	CF	10	6.8	220	1.18	9.5 ± 0.7
No. 3	Normal PA66	GF	15	7.4	145	1.25	5.9 ± 0.3
No. 4	High molecular mass PA66	GF	15	7.4	193	1.25	6.0 ± 0.4
No. 5	Normal PA66	GF	33	18.3	145	1.39	10.7 ± 0.3
No. 6	Normal PA66	-	-	-	145	1.14	3.0 ± 0.1

2.2 Steel cylinders

The steel cylinders used for the sliding tests explained in Section 2.4 were fabricated from S45C steel, which contained 0.45 wt.% carbon, following JIS G 4051 (Japanese Industrial Standards). The roughness of the sliding surface was S_a 0.2 μm, which was obtained using a centerless grinding process, and the steel had a hardness of 4.5 GPa (no heat treatment). In addition, steel cylinders with various hardness were prepared using different heat

treatment conditions (quenching and tempering), as listed in Table 2, to investigate the effect of the steel hardness, as presented in Section 3.4. The hardness of the steel cylinders was measured via micro-indentation, using a Vickers indenter with a normal load of 300 mN. The details of the heat treatment conditions and microstructure are shown in Fig. S1 and S2 in the supplementary material.

Table 2 Heat treatment conditions for the steel cylinders.

Quench hardening	Tempering	Hardness measured through micro-indentation (GPa)
- (Raw steel)	-	4.5 ± 0.1
890 °C for 30 min, oil cooling	412 °C for 60 min, air cooling	5.4 ± 0.2
	300 °C for 60 min, air cooling	7.2 ± 0.1

2.3 Grease

Table 3 lists the grease compositions used for the sliding tests under grease lubrication. Each sliding test (described in Section 3.2-3.4) was conducted using grease no. 1, which consisted of poly- α -olefin 8 (PAO8) as the base oil, diurea as a thickener, zinc carboxylate as a low friction agent, and a sulfur type anti-oxidation agent (the detailed composition of the grease can be found in Ref. [12]). The zinc carboxylate was composed of various metal carboxylates, such as palmitate and stearate. To elucidate the tribochemical reaction mechanism, a grease without zinc carboxylate (no. 2) was also evaluated, as explained in Section 3.4.

Table 3 Compositions of the evaluated greases.

Sample number	Base oil	Thickener	Low friction agent	Anti-oxidation agent
No. 1	PAO8	Diurea	Zinc carboxylate	Sulfur type agent
No. 2	PAO8	Diurea	-	Sulfur type agent

2.4 Experimental setup, measurements, and observations

The tensile mechanical properties of the evaluated PA66 and fiber-reinforced composites were measured according to the standard ISO527; Table 4 lists the tensile test conditions.

Table 4 Test conditions for the tensile tests.

Tensile test specimens	Shape	150 mm × 10 mm × 4 mm
Test conditions	Tensile speed	5 mm/s
	Temperature	25 °C, 120 °C
Measured data		- Tensile strength - Young's modulus -Tensile elongation at break

To discuss the effect of the relationship between the hardness of the steel counterpart and that of the reinforcement fibers on the tribological properties, the hardness of a single fiber was measured using the following process. First, cut strands of fiber were embedded in an epoxy resin in the perpendicular and horizontal directions, as presented in Fig. 1, and the epoxy resin was cured. Then, the surface of the epoxy resin was polished and the hardness of the fibers was measured using nanoindentation; measurement was performed with a Berkovich indenter and normal loads of 4,000 μN for the GFs and 4,000 – 13,000 μN for the CFs.

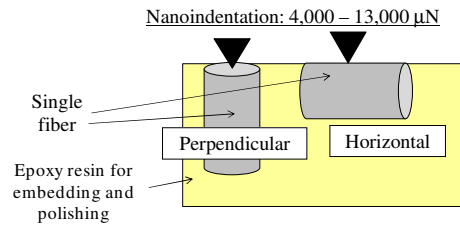


Fig. 1 Schematic of the nanoindentation hardness measurements of fibers.

The tribological properties were evaluated via sliding tests without (dry) or with grease lubrication, using a rotating PA66 or composite ring in contact with four fixed steel cylinders, which was the same contact geometry as applied in the authors' previous studies [11–13, 27]. The test specimens used for the sliding tests and the tribometer setup are shown in Fig. 2. The ring specimens were cut to 3 mm in height using a lathe; then, the sliding surface was polished with #600 emery paper before conducting the sliding tests, leading to a roughness of Sa 0.5 μm . The sliding tests were performed for intermittent durations (1 s, 20 s, and 200 s) to control sliding heat generation. When the tests were performed under grease lubrication, 0.85 g of grease was prepared in the sample holder for each test. A normal load was applied using dead weights. The weight and height of each PA66 or composite ring specimen were measured before and after each sliding test to estimate the wear and creep separately. The total height loss (h_{total} , the height difference of the ring specimen before and after the sliding tests) was the summation caused by creep and wear, whereas the wear height loss (h_{wear}) was calculated from the wear mass of the ring specimen (M_{wear}), the density of the PA66 or composite (d), and the sliding surface area (s , approximately 200 mm^2) using the following equation:

$$h_{wear} = \frac{M_{wear}}{ds} \quad (1)$$

The creep height loss (h_{creep}) was estimated by subtracting h_{wear} from h_{total} .

$$h_{creep} = h_{total} - h_{wear} \quad (2)$$

Furthermore, the vertical displacement of the steel cylinders sample holder was directly measured during the sliding tests. During the tests, the temperature of the steel cylinder holder was measured using a thermocouple. For the sliding tests conducted at higher temperatures, two cartridge heaters were inserted into the sample holder of the steel cylinders and the sample holder and steel cylinder were heated. The friction torque (T) was measured with a force sensor and the friction coefficient (μ) was calculated using the normal load (N) and mean rotation radius (r , 11.4 mm).

$$\mu = \frac{T}{rN} \quad (3)$$

One cycle in this sliding test consisted of one rotation of the composite ring. Table 5 lists the sliding test conditions. The normal load is set to simulate the high contact pressure observed in the actual worm reducer of electric power steering and to allow comparison of the tribological properties of different materials in a short time.

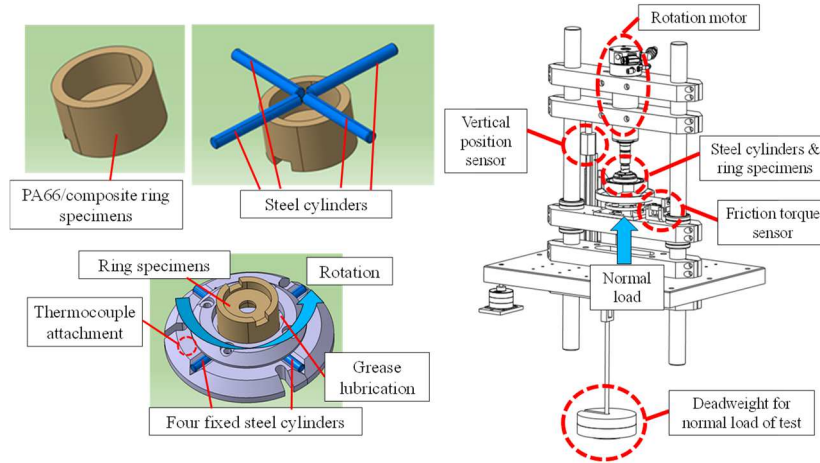


Fig. 2 Schematics of the test specimens and the sliding test setup.

Table 5 Test conditions for the sliding tests.

Steel cylinders (×4)	Diameter	3.5 mm			
	Length	30 mm			
PA66 ring (JIS K 7218)	Outer diameter	25.6 mm			
	Inner diameter	20 mm			
	Height	12 mm			
Test conditions	Rotation speed	790 rpm			
	Mean sliding speed	1 m/s (Mean radius of the contact area: 11.4 mm)			
	Normal load	120 N	220 N	350 N	220-350 N
	Test duration	10.8-73.8 min: intermittent process (10 s sliding and 1 s stopping)	240 min: intermittent process (10 s sliding and 20 s stopping)	15.6-117 min: intermittent process (10 s sliding and 1 s stopping)	0.4-47.1 h: intermittent process (10 s sliding and 200 s stopping)
	Total sliding cycles	7,575-51,698	61,760	10,946-82,165	1,018-104,114
	Total sliding duration	9.8-67.1 min	80 min	14.2-106.4 min	1.2-134.7 min
	Environment temperature	25 °C	25 °C	25 °C	25-80 °C

	Lubrication	Dry	Grease	Grease	Grease
Evaluated polymer specimens (in Table 1)		No. 1, 3, 6 (Section 3.1)	No. 1, 3 (Section 3.3)	No. 1, 2, 3, 4, 5, 6 (Section 3.2 and 4 in supplementary material)	No. 1, 3, 5 (Section 3.4)

2.5 Microscopy and surface analysis

After the sliding tests, the specimens were washed using an ultrasonic bath containing a heptane solvent to remove the grease on the sliding surface and surface observations and analysis were conducted. The sliding surfaces of the ring specimens and the shape of the wear debris, particularly under dry conditions, were observed with an optical microscope. The sliding surfaces of the steel cylinders were observed via scanning electron microscopy (SEM); interferometry was also used to observe the wear scars on the steel cylinders and evaluate the wear volume after the tests. X-ray dispersive spectroscopy (EDX) was conducted to determine the composition of the tribofilm on the sliding surface of the ring specimens. In addition, to consider the effects of the fiber orientation on the wear of the composite and steel, the fiber orientation on the sliding surface of the new CF composite ring specimen (sample no. 1) was observed through SEM and analyzed via image analysis in the same manner as described in the authors' previous work [11]. The detailed procedures and results are described in the supplementary material (see Fig. S3 – S6).

3. Results and Discussion

3.1 Tribological properties without lubrication

First, the tribological properties under dry conditions were investigated using the contact geometry described in Section 2.4 to understand the difference in the tribological behavior of the unreinforced PA66 and fiber-reinforced composites, with and without grease lubrication. Fig. 3 presents the evolution of the friction coefficient, temperature, and vertical displacement of the PA66 composite with 10 wt.% CF (sample no. 1 in Table 1), the PA66 composite with 15 wt.% GF (no. 3), and the unreinforced PA66 (no. 6) under a normal load of 120 N and dry conditions during 7,575 – 51,968 cycles, using the steel cylinders with a hardness of 4.5 GPa; an intermittent process was used, i.e., sliding for 10 s followed by stopping for 1 s. The sliding tests were conducted at least twice for each material under the same normal load. The weight fraction of fibers was different between samples no. 1 and no. 3; however, the volume fraction of the fibers was similar (6.8 % and 7.4 %, respectively) because of the density difference of the GFs and CFs, as listed in Table 1. In addition, the CF 10 % composite and GF 15 % composite had approximately the same total fiber area on the sliding surface (see Fig. S5 in the supplementary material). Fig. 4 presents the optical microscope observations of the surface of the ring specimens and wear debris after the sliding tests, along with the weight, creep, and total height loss estimated using the method presented in Section 2.4. The friction coefficient in this test using the CF composite was lower than that of the GF composite. The average friction coefficient using the CF composite (up to 20,000 cycles) was 0.230 ± 0.055 and that of the GF composite was 0.306 ± 0.025 (33.0 % higher). In addition, the average friction coefficients using the CF and GF composites from 15,000 – 20,000 cycles (after each value became stable) were 0.256 ± 0.022 and 0.305 ± 0.010 , respectively. This indicates that the stabilized friction coefficient using the GF-reinforced composite was 19.4 % higher than that of the CF-reinforced composite.

High friction coefficient induces sliding heat generation and, thus, high temperature; the CF-reinforced composite exhibits a lower friction coefficient and temperature than the GF composite. A sudden large increase in the vertical displacement was observed in the GF composite at 21,000 – 23,000 cycles and was more closely related to the plastic deformation (creep) of the composite caused by the high friction coefficient, high temperature, and shear stress than the wear of the composite, considering that the composite ring lost very little weight (i.e., the wear of the composite) and almost no wear debris was observed after 21,000 – 23,000 cycles. In contrast, a gradual increase in the vertical displacement caused by the wear was observed in the CF composite while the sudden increase in the displacement (as observed in the GF composite) did not occur. Unlike the GF composite, 88 % of the height loss was caused by wear and only 12 % was caused by creep, after 51,968 cycles. Wear debris was observed, which had an indefinite shape (including fibers). These results indicate that the CF composite did not have superior wear resistance compared to the GF composite under these test conditions, despite its lower friction coefficient; however, the lower friction coefficient reduced the amount of heat generated and prevented the plastic deformation of the CF composite. In contrast, the friction coefficient and temperature of the unreinforced PA66 became higher than the GF and CF composites and the rate of increase in the vertical displacement was also high. The difference in the temperature cannot be related to the difference in the thermal conductivity of evaluated materials because the difference in the thermal conductivity is negligible; 0.32 W/mK for the unreinforced PA66, 0.36 W/mK for the GF composite, and 0.34 W/mK for the CF composite. CF is known to exhibit high (10 W/mK) thermal conductivity [24]; however, short CFs have difficulty forming a thermal conductive pass inside the molding compact. Therefore, the difference in temperature evolution is not related to the difference in thermal conductivity but it is related to the difference in the friction coefficient. The generation of fibrous wear debris was observed and a sudden increase in the displacement related to creep (plastic deformation) was observed after 8,300 cycles. This indicates that the addition of the reinforcement fibers reduced the friction and improved the tribological properties, and the diminishing effect of the friction coefficient in the CF composite was much larger than that in the GF composite under the dry test condition in this contact geometry.

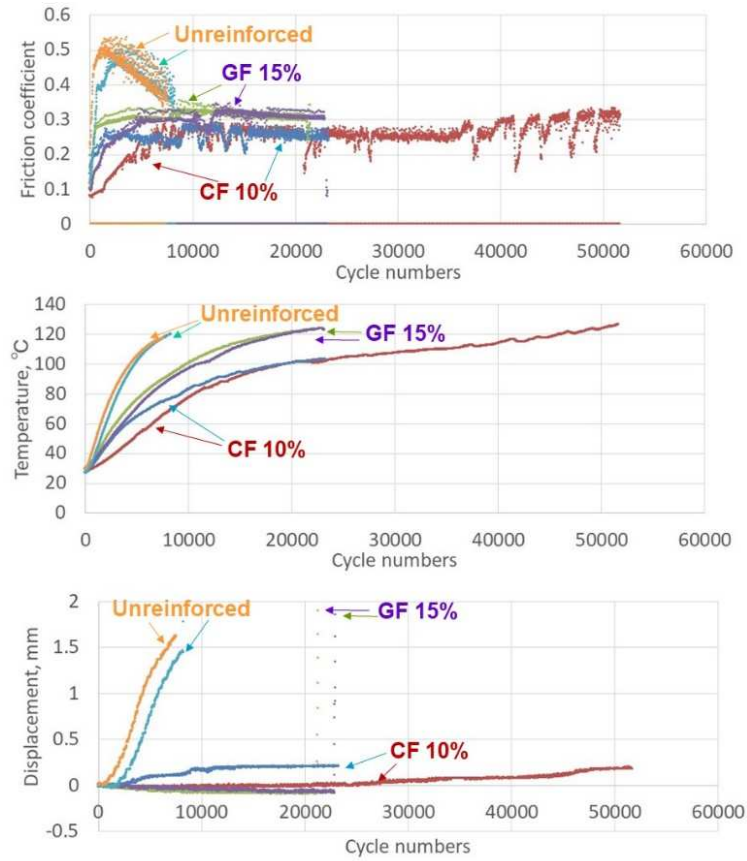


Fig. 3 Evolution of the (a) friction coefficient, (b) temperature, and (c) vertical displacement during the sliding tests under dry conditions and a normal load of 120 N, with sliding for 10 s followed by stopping for 1 s.

	Unreinforced PA66 7,575 cycles (before sudden increase in the displacement)	Unreinforced PA66 8,332 cycles (after sudden increase in the displacement)	GF 15% composite 21,528 cycles	CF 10% composite 51,968 cycles
Entire ring surfaces				
Magnified ring images				
Wear debris			Almost no wear debris	
Wear height loss	0.934 mm	0.987 mm	0.050 mm	0.255 mm
Creep height loss	0.716 mm	1.575 mm	3.178 mm	0.023 mm
Total height loss	1.650 mm	2.562 mm	3.228 mm	0.278 mm

Fig. 4 Optical microscope observations of the ring specimens and wear debris, and the wear/creep/total height loss of the unreinforced PA66 after 7,575 and 8,332 cycles, GF 15 % composite after 21,528 cycles, and CF 10 % composite after 51,968 cycles of the sliding tests under dry conditions and a normal load of 120 N.

Fig. 5 presents the optical microscope observations of the steel cylinder after testing for 7,575 cycles with the unreinforced PA66, 21,528 cycles with the GF 15 % composite, and 23,249 cycles with the CF 10 % composite, under the same test conditions. The steel cylinders were washed using an ultrasonic bath with a heptane solvent before the observations. The sliding surface was brown after testing with the GF composite and black wear debris was attached to the edge of the sliding surface after testing with the CF composite; in contrast, explicit wear scars and the attachment of wear debris were not observed after testing with the unreinforced PA66. The wear volume of the steel cylinder tested with the CF composite was higher than that of the cylinder tested with the GF composite. Fig. 6 shows the SEM observations and SEM-EDX analysis of the cylinder tested with the GF composite or CF composite. Severe wear scars in the sliding direction, which are generally caused by two-body abrasive wear, were observed on the surface of both steel cylinders. In addition, some dark patches were observed on the surface of the cylinder tested with the GF composite; they were composed of carbon and oxygen, indicating that they originated from the PA66 and silicon (which was present in the GFs). Therefore, portions of the GF composite were strongly adhered to the steel sliding surface, even after ultrasonic washing. Carbon was detected via SEM-EDX analysis on the sliding surface of the CF composite test cylinder and the edge of the wear scar. Therefore, the CF composite also adhered to the steel surface. This indicates that the wear mode of both composites under dry conditions was adhesive wear.

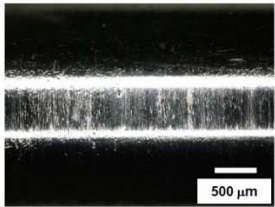
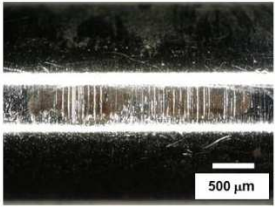
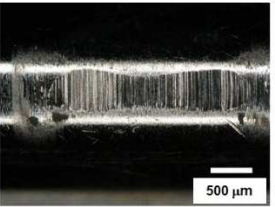
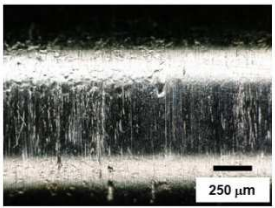
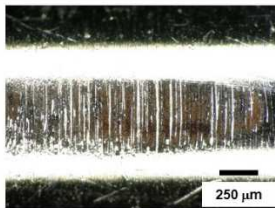
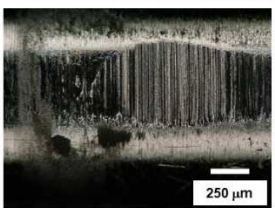
Magnification	Tested with unreinforced PA66 for 7,575 cycles	Tested with GF composite for 21,528 cycles	Tested with CF composite for 23,249 cycles
x100			
x200			
Wear volume via interferometry	-	0.0097 mm ³	0.0313 mm ³

Fig. 5 Optical microscope observations of the steel cylinder surface after the sliding tests.

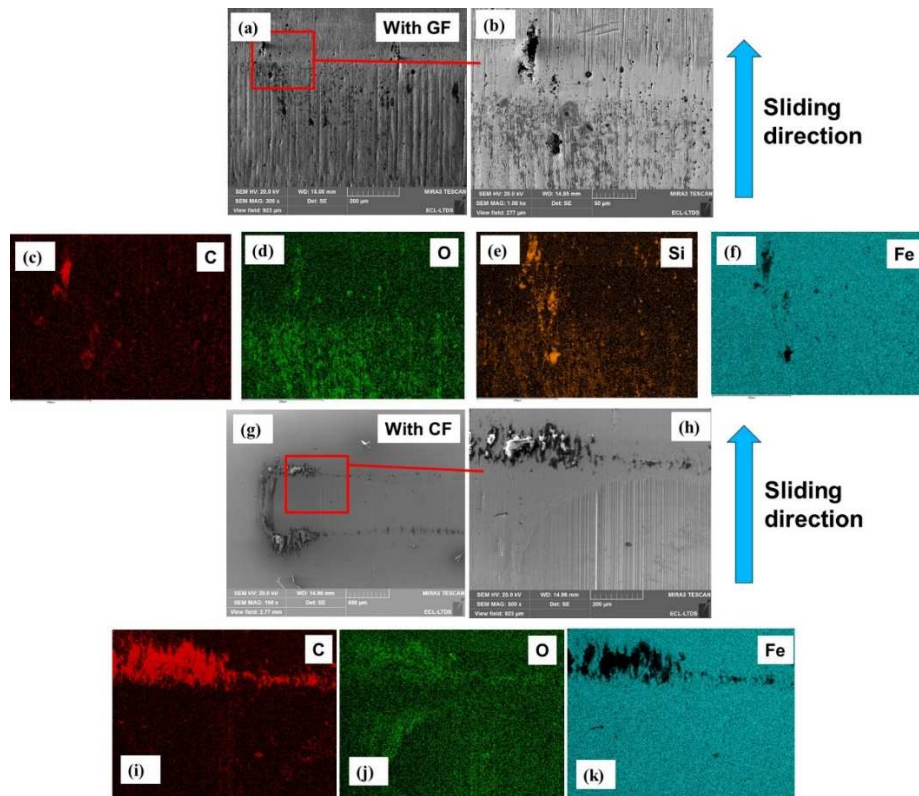


Fig. 6 (a) and (b) SEM observations of the steel cylinder tested with the GF composite after 21,528 cycles; (c) – (f) SEM-EDX images of the carbon, oxygen, silicon, and iron content at the same location as the SEM image in (b); (g) and (h) SEM observations of the steel cylinder tested with the CF composite after 23,249 cycles; and (i) – (k) SEM-EDX images of the carbon, oxygen, and iron content at the same location as the SEM image in (h).

The low friction characteristics of the CF-reinforced composite under dry conditions compared to GF composites and unreinforced PA66 were reported in several previous works [17, 25, 26, 28]. The wear mode of the polymer under dry conditions is explained primarily as adhesive wear and the friction coefficient and wear behavior of the polymer are strongly affected by the formation of a transfer film on the metallic surface. This transfer film prevents adhesion between the polymer and metallic surface and reduces the plowing action of metallic asperities on the soft polymer surface [29]. In addition, under dry conditions, the reinforcement fibers contribute significantly to the reduction in the adhesive effect by reducing the real contact area between the metallic surface and polymeric surface. CF is graphitized carbon with the hexagonal planes of its crystals aligned perpendicular to the fiber axis. The lubricating function of the graphitized carbon, in which the graphite debris form a thin lubrication film on the counter-face, is thought to be responsible for the reduction in the friction coefficient when CF composites slide against steel [30, 31]. Therefore, a larger reduction in the friction coefficient results in a smaller temperature increase and the smaller wear amount in the CF composite compared to the GF composite is attributed to the formation of a low friction transfer film on the counterpart steel.

In summary, the CF composite exhibited better tribological properties even under a higher contact pressure than the unreinforced PA66 or GF-reinforced PA66 composite when sliding in contact with the carbon steel under dry conditions.

3.2 Tribological behavior under grease lubrication

Sliding tests using the GF 15 % composite (sample no. 3) under grease lubrication were conducted with a normal load of 120 N (the same load that was used for the dry conditions presented in Section 3.1); however, no change in the vertical displacement (wear or creep of the composite) was observed, even after 1,200,000 cycles (see Fig. S7 in the supplementary material). For comparison, severe plastic deformation of the GF composite was observed after just 21,000 – 23,000 cycles under dry conditions and the same contact pressure condition, as presented in Fig. 3. Therefore, the grease lubrication improved the durability of the GF composite by a factor of at least 60. To compare the difference in the wear and creep resistance of the composite under grease lubrication, sliding tests with a higher normal load (350 N) were conducted.

Fig. 7 presents the evolution of the friction coefficient, temperature, and vertical displacement for a normal load of 350 N under grease lubrication (during the initial 10,000 cycles and the entire test) using the same plastic material and steel cylinder used in Section 3.1. The Hertzian contact pressure, calculated using Young's modulus at room temperature, was higher for the CF 10 % composite than for the GF 15 % composite and than for the unreinforced PA66. Sliding tests were conducted at least twice for each material. Completely different tribological properties were observed under grease lubrication compared to those observed under dry conditions (which were dominated by adhesion). During the initial 5,000 cycles, the friction coefficient, temperature, and vertical displacement of the unreinforced PA66 exhibited higher values than those of the GF- or CF-reinforced composites. However, sudden increases in the vertical displacement and the friction coefficient were observed in the fiber-reinforced composites, as described in the authors' previous study [11]. Unlike under dry conditions, the tribological properties of the CF 10 % composite were poorer than those of the GF 15 % composite; the sudden increases in the friction coefficient and the vertical displacement occurred at earlier cycles for the CF 10 % composite and the rate of increase in the displacement was higher. The volume fraction of fibers in the GF 15 % composite and CF 10 % composite was similar while Young's modulus of the CF 10 % composite was higher than that of the GF 15 % composite. Therefore, the higher Young's modulus and contact pressure of the CF 10 % composite might induce the deterioration in the tribological properties. Thus, a sliding test of the GF 33 % composite (sample no. 5), which had a similar Young's modulus (10.7 GPa) to the CF 10 % composite (9.5 GPa), was also conducted to compare the tribological properties under similar contact pressures, as presented in Fig. 7. The Hertzian contact pressure of the GF 33 % composite at room temperature was 252 MPa, which was slightly higher than that of the CF composite. The sudden increase in the vertical displacement in the GF 33 % composite (10,000 – 21,000 cycles) occurred earlier than in the GF 15 % composite (19,000 – 23,000 cycles) and the rate of the increase in the displacement was higher. Nevertheless, the sudden increase in the vertical displacement in the GF 33 % composite still occurred later than it did in the CF 10 % composite (9,000 – 11,000 cycles) and the rate of increase in the vertical displacement and absolute value of the displacement in the GF 33 % composite were lower than those in the CF 10 % composite. This indicates that the tribological properties of the CF composite were also poorer than those of the GF 33 % composite, even with a similar contact pressure. The wear mode of the composite under dry conditions was adhesive and the addition of the CFs prevented adhesion to the steel counterpart and provided lubrication. However, the effect of adhesion was weak under grease lubrication because direct contact between the PA66 and steel counterpart was prevented and low friction was ensured by

the grease, not by the presence of fibers.

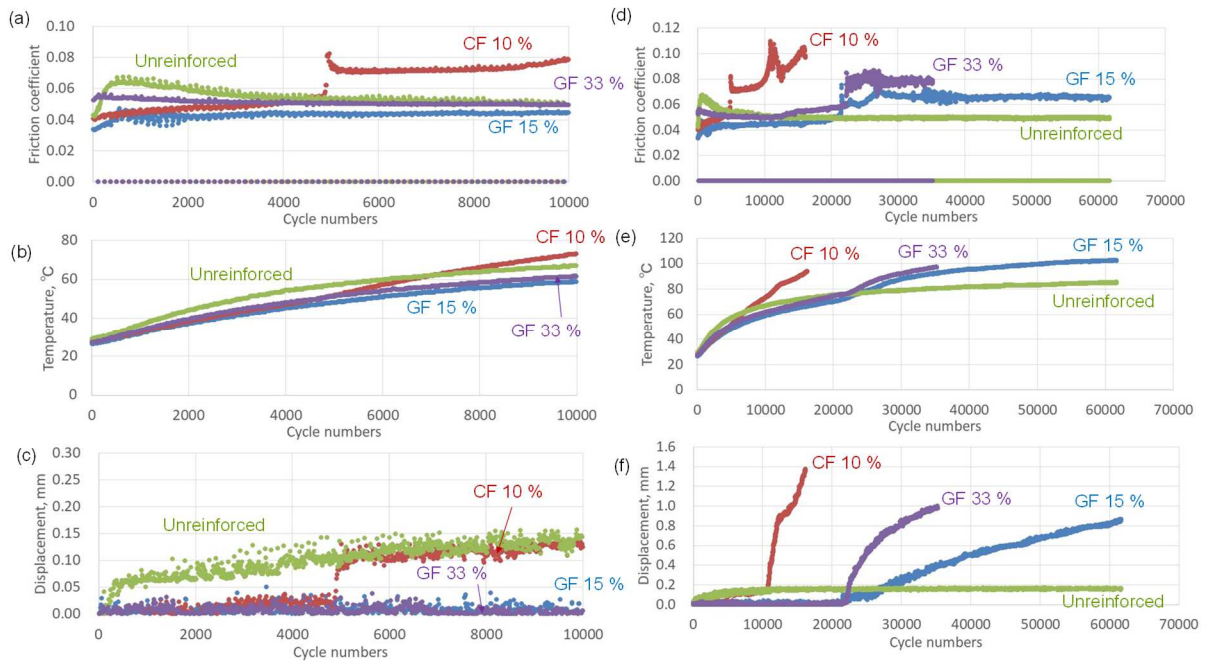


Fig. 7 Evolution of the (a) friction coefficient, (b) temperature, and (c) vertical displacement during the first 10,000 cycles, and the (d) friction coefficient, (e) temperature, and (f) vertical displacement during the entire duration of the sliding tests under grease lubrication and a normal load of 350 N.

Fig. 8 presents the optical microscope observations of the sliding surface of the ring specimens and the wear/creep/total height loss of the ring specimens estimated using the method explained in Section 2.4. In contrast to dry conditions, the height loss due to wear of the unreinforced PA66 was relatively small and 75 % of the total height loss was due to creep. No severe wear on the sliding surface was observed. However, wear had a larger effect than creep, and the entire sliding surface was severely damaged for the CF and GF composites. The damage mode of the GF composite, which is two-body abrasive wear related to peeling fibers that detach and scratch the PA66, was reported in the authors' previous study [11] and the same wear mode was observed for the CF composite, including the exposure of fibers (peeling) on the sliding surface. To understand the difference in the tribological properties between the GF composite and CF composite under grease lubrication more deeply, the effect of the PA66 molecular mass (Section 4 in the supplementary material), hardness of the steel counterpart (Section 3.3), and the temperature (Section 3.4) were investigated.

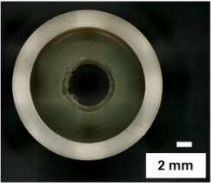
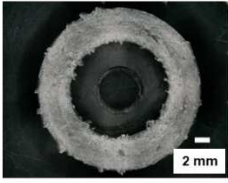
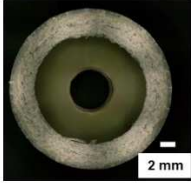
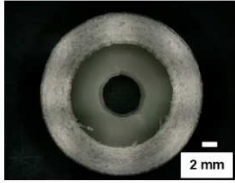
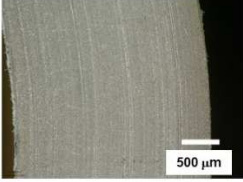
	Unreinforced PA66 after 61,704 cycles	CF 10% composite after 16,186 cycles	GF 15% composite after 61,665 cycles	GF 33% composite after 35,242 cycles
Entire sliding surface				
Magnified image				
Wear height loss	0.023 mm	0.501 mm	0.575 mm	0.521 mm
Creep height loss	0.062 mm	0.765 mm	0.242 mm	0.465 mm
Total Height loss	0.085 mm	1.266 mm	0.817 mm	0.986 mm

Fig. 8 Optical microscope observations of the sliding surface and the wear/creep/total height loss after the sliding tests.

3.3 Effects of the hardness of the counterpart steel on the tribological properties and clarification of the wear mechanism of the steel counterpart

Fig. 9 presents the effect of the hardness of the counterpart steel on the wear and creep height loss of the composite, as well as the wear volume of the steel cylinder measured via interferometry for a normal load of 220 N (lower than the conditions presented in Section 3.2) after 61,700 cycles (sliding for 10 s followed by stopping for 20 s) under grease lubrication using the CF 10 % composite (no. 1) and GF 15 % composite (no. 3). The Hertzian contact pressure based on the Young's modulus at room temperature was higher for the CF 10 % composite than for the GF 15 % composite. As the hardness of the steel increased, the wear of the composite increased and the wear of the steel decreased. This trend coincides with the authors' previous work on the tribology of a GF-reinforced PA66 composite for a normal load of 350 N [11] and it was explained by the relationship between the hardness of the counterpart steel and GFs; using steel with a hardness lower than the hardness of the GFs increased the wear of the steel counterpart, whereas the wear of the GF composite decreased. The wear and creep of the CF composite were higher than those of the GF composite regardless of the steel hardness; this is the same trend observed in the results from the tests with a normal load of 350 N (as explained in Section 3.2). In addition, the steel wear decreased as the steel hardness increased and the steel wear was 4.5 – 67 times higher when tested using the CF composite than it was when tested using the GF composite, regardless of the hardness of the steel cylinder. This trend completely differs from the other works presented in Section 1.

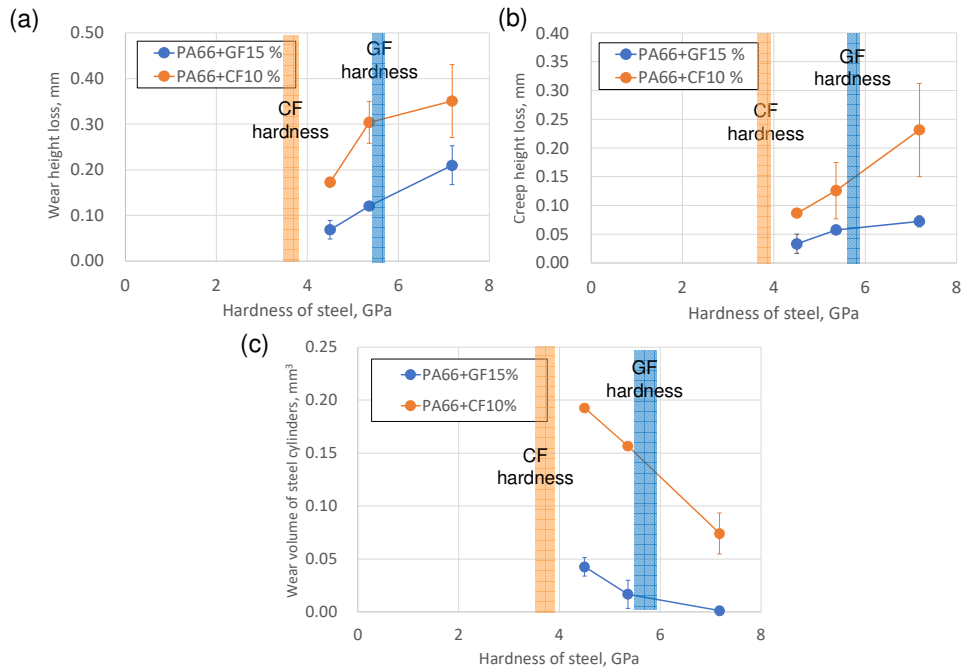


Fig. 9 Relationship between the hardness of steel cylinders and (a) the decrease in the weight of the composite ring; (b) the creep height loss of the composite ring; and (c) wear volume of the steel cylinders after 61,700 cycles of the sliding test for a normal load of 220 N with sliding for 10 s followed by stopping for 20 s.

Fig. 10 shows the evolution of the friction coefficient, temperature, and vertical displacement in the sliding tests using the GF and CF composites and steel cylinders with a hardness of 4.5 GPa as a representative example. The friction coefficient and vertical displacement began to increase at 5,000 cycles for the CF composite, whereas no sudden increase was observed up to 35,000 – 40,000 cycles for the GF composite. In addition, the friction coefficient, temperature, and vertical displacement in the CF composite exhibited higher values than those of the GF composite after 5,000 cycles until the end of the test. Fig. 11 shows the optical microscope observations of the ring surface after 61,700 cycles for the tests using steel counterparts with different values of hardness and composites with different fibers. The damage to the ring sliding surface increased as the hardness of the steel increased.

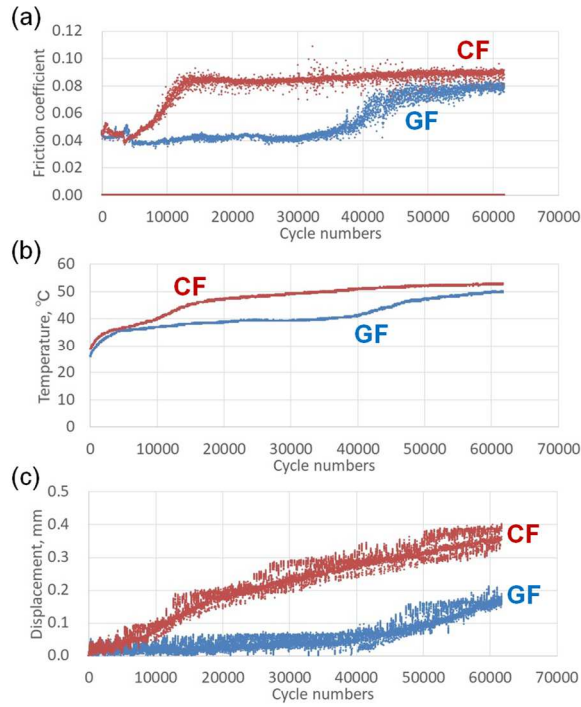


Fig. 10 Evolution of the (a) friction coefficient, (b) temperature, and (c) vertical displacement in the sliding tests under grease lubrication for a normal load of 220 N with sliding for 10 s, followed by stopping for 20 s using steel cylinders with a hardness of 4.5 GPa.

Hardness of the counterpart steel	4.5 GPa	5.4 GPa	7.2 GPa
PA66+GF15 %			
PA66+CF10 %			

Fig. 11 Optical microscope observations of the ring surfaces after 61,700 cycles of the sliding test using steel counterparts with different hardness and composites with different fibers.

To understand the effect of the steel hardness on the tribological properties, the hardness of the GFs and CFs were measured using the method presented in Section 2.4. Fig. 12 shows an atomic force microscope (AFM) image of the steel surface after the hardness measurements for a normal load of 13,000 μN , the hardness of the GFs and CFs measured at various positions for a normal load of 4,000 μN , and the effect of the normal load used for the nanoindentation on the measured hardness of the CFs oriented in the perpendicular direction. The indentations were not clearly visible on the surface of the CF (even those made under a maximum load of 13,000 μN). The hardness of the CFs oriented in the perpendicular direction was 3.9 ± 1.0 GPa for a normal load of 4,000 μN and minimal variation in the hardness was observed for different normal loads. This value is similar to that reported in [32] (i.e., 2.5 – 5 GPa). The hardness of the GFs in the perpendicular direction for a normal load of 4,000 μN was 5.7 ± 0.2 GPa; therefore, the hardness of the CFs was 35 % lower than that of the GFs in the perpendicular direction. In addition, anisotropy in the hardness of the CFs was observed, whereas the measured direction did not affect the hardness of the GFs. The hardness of the CFs in the perpendicular direction for a normal load of 4,000 μN was 1.61 times higher than that in the horizontal direction. The anisotropy of the mechanical properties (Young's modulus and the hardness) of the CFs was also presented by Sun et al. [33], and the mechanical properties of the CFs in the transverse section (perpendicular direction) were higher than those in the longitudinal section (horizontal direction). The difference in the anisotropy between the GFs and CFs is due to the differences in the molecular structure of the fibers. CFs have high crystallinity and the c-axis of the graphite crystallites is perpendicular to the fiber axis [26]; therefore, the hardness of the CF in the perpendicular direction is higher than in the horizontal direction. In contrast, GFs have an amorphous structure, which has no anisotropy; therefore, the measurement position does not affect the hardness of the GFs.

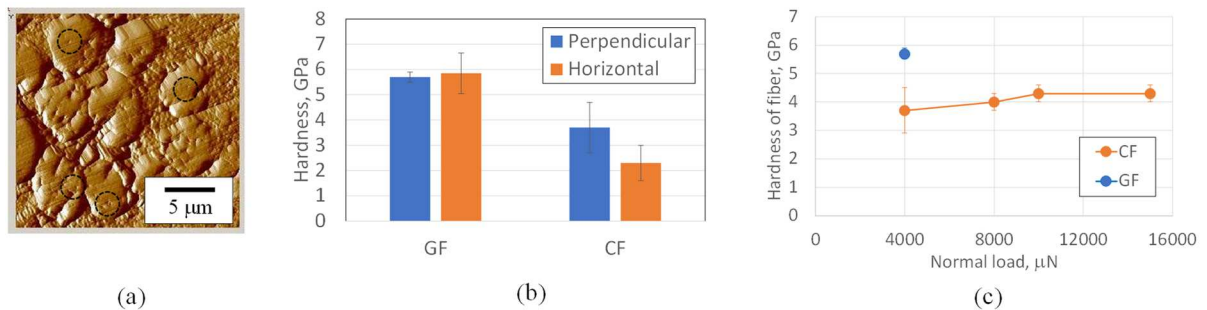


Fig. 12 (a) AFM image of the CFs after the hardness measurements with a normal load of 13,000 μN , (b) the hardness of the GFs and CFs measured at various positions with a normal load of 4,000 μN , and (c) the effect of the normal load of the nanoindentation on the measured hardness of the CFs oriented in the perpendicular direction.

The results of the sliding tests and hardness of the fibers indicate that the CFs were softer than the steel cylinder, with the lowest hardness (4.5 GPa measured by micro-indentation), even after considering the anisotropy of the CF hardness. In addition, there were no significant differences in the fiber area on the sliding surface of the composite ring between the CF 10 % composite (sample no. 1) and GF 15 % composite (sample no. 3), as presented in Fig. S5 in the supplementary material. This indicates that the destructive effects of the composite on the counterpart steel under grease lubrication were not determined solely by the difference in the

hardness of the fibers and steel because the destructive effects of the CF composite on the counterpart steel were higher than those of the GF composite for all steel hardness. Therefore, the wear resistance of the counterpart steel is related to the wear resistance of the composite, which is related to the interfacial adhesion between the PA66 and fibers (considering that increasing the molecular mass of the PA66 in the CF composite improved the wear resistance of both the composite and the counterpart steel, as presented in Section 4 in Supplementary material). Hence, the difference in the adhesion between the fibers and PA66 was investigated.

The fracture surface on the composite in the tensile test was observed to compare the interfacial adhesion between the fibers and the PA66. Fig. 13 presents the SEM observations of the fracture surfaces from the tensile tests at 120 °C with the GF 15 % and CF 10 % composites (samples no. 4 and no. 2, respectively). The elongation at break at 120 °C of the GF composite was 3.5 times higher than that of the CF composite ($21.3 \pm 0.6 \%$ and $6.4 \pm 0.3 \%$, respectively). In the GF composite, few gaps between the PA66 and GFs in the perpendicular direction were observed and the GFs strongly adhered to the entire surface of the PA66. In contrast, numerous gaps between the CFs and PA66 were observed in the CF composite and the CFs were exposed without adhesion to the PA66, even when the PA66 could undergo further elongation. These observations clearly demonstrate the difference in the interfacial adhesion between the PA66 and the GFs and CFs, and the difference in the elongation at break between the GF and CF composites. The schematics in Fig. 14 illustrate the differences in the sliding behavior of the CF and GF composites in contact with the carbon steel counterpart considering the differences in the interfacial adhesion between the PA66 and the fibers. The weak interfacial shear strength between the CFs and PA66 induces the gap between the CFs and PA66 on the sliding surface, leading to the exposure of the acute CF edges (which exhibit greater destructive effects on the steel than the smooth surface of the CF) and the wear of the steel counterpart. In addition, scratches on the PA66 propagate from the gap between the PA66 and CF, leading to an increase in the amount of wear on the composite. In contrast, the good interfacial adhesion between the GFs and PA66 prevents exposure of the GF edges, which have highly destructive effects on the steel counterpart, and reduce the wear of the steel. In addition, the fewer gaps between the GFs and PA66 prevent the generation of scratches on the PA66, leading to a smaller amount of wear on the composite. In summary, one cause of the difference in the wear resistance between the GF composite and CF composite is the difference in the interfacial adhesion between the fibers and PA66.

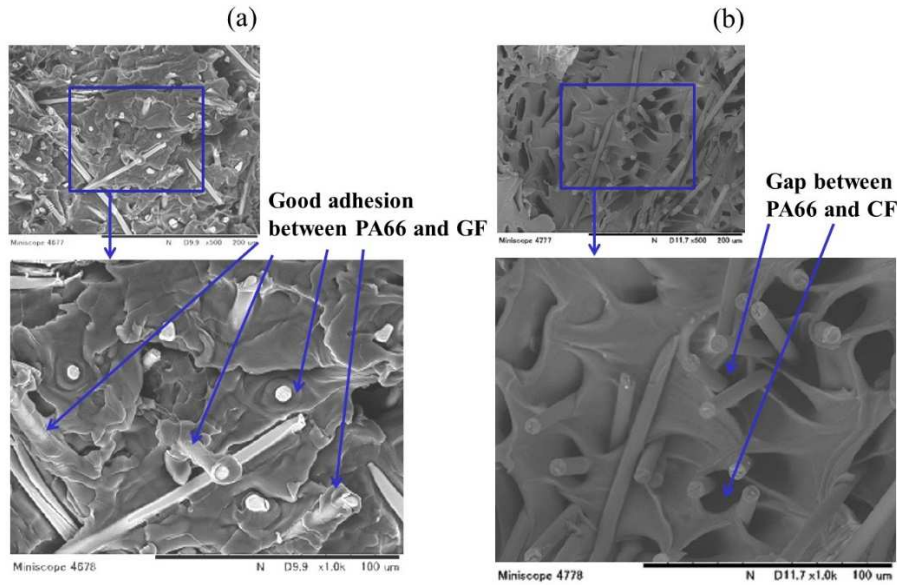


Fig. 13 SEM observations of the fracture surfaces from the tensile tests at 120 °C of the (a) PA66 composite with 15 % GF and (b) PA66 composite with 10 % CF.

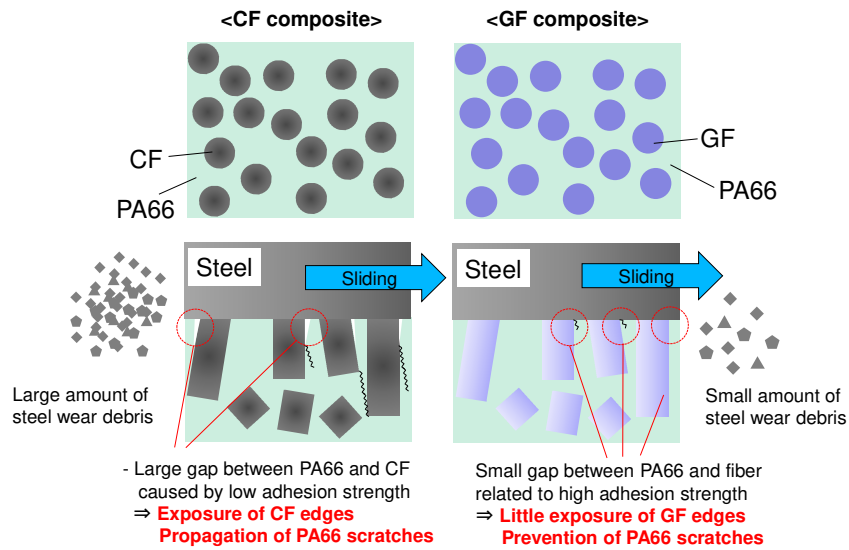


Fig. 14 Schematics of the differences in the sliding behavior of the GF composite and CF composite.

3.4 Differences in the temperature dependence of the tribological properties and tribochemistry between the CF and GF composites

In the authors' previous study [12], the effects of additives in the grease (zinc carboxylate and sulfur type anti-oxidation agents) on the tribological properties of GF-reinforced PA66 in contact with steel were investigated. In the present study, the tribochemistry of the CF-reinforced composite was investigated and compared to the reported mechanism in the GF-reinforced PA66 composite. Fig. 15 presents the evolution of the friction coefficient and vertical displacement using the normal molecular mass CF 10 % composite (sample no.

1 in Table 1) and GF 15 % composite (sample no. 3) with the grease containing zinc carboxylate (sample no. 1 in Table 3) under a normal load of 350 N, with sliding for 10 s followed by stopping for 200 s (the test was performed at a stable temperature by preventing sliding heat generation with the introduction of a long stopping phase) at room temperature and 80 °C. Optical microscope observations of the sliding surfaces after the sliding tests are shown in Fig. S15 in the supplementary material. The GF composite generally exhibited better tribological properties at 80 °C than at room temperature; however, no significant difference was observed. In contrast, the CF composite exhibited the opposite trend: the tribological properties at room temperature were better than those at 80 °C and the sudden increases in the friction coefficient and displacement occurred after more cycles at room temperature than at 80 °C. Fig. 16 shows the wear and creep of the composite and wear of the steel cylinders (the total wear of the four steel cylinders). No significant differences in the wear and creep of the GF composite or the wear of the steel cylinders tested with the GF composite were observed between room temperature and 80 °C. In contrast, the wear and creep of the CF composite at 80 °C were considerably higher than those at room temperature, and the wear volume of the steel cylinders tested with the CF 10 % composite at 80 °C was 1.9 times higher than that at room temperature. Considering the difference in the tribological properties between the GF 15% composite and CF 10% composite, the wear of the GF 15 % composite was much lower than that of the CF 10 % composite at both room temperature and 80 °C; thus, this trend is the same as that observed in Section 3.3. The wear of the steel cylinders tested with the CF 15 % composite was also 3.5 and 6.5 times higher than those tested with the GF 10 % composite at room temperature and 80 °C, respectively, even though the hardness of the CF itself was much lower than that of the GFs. This trend is also the same as that observed in Section 3.3 and these results also explain why the wear of the counterpart steel cannot be determined solely by the hardness of the reinforcement fibers for sliding under grease lubrication.

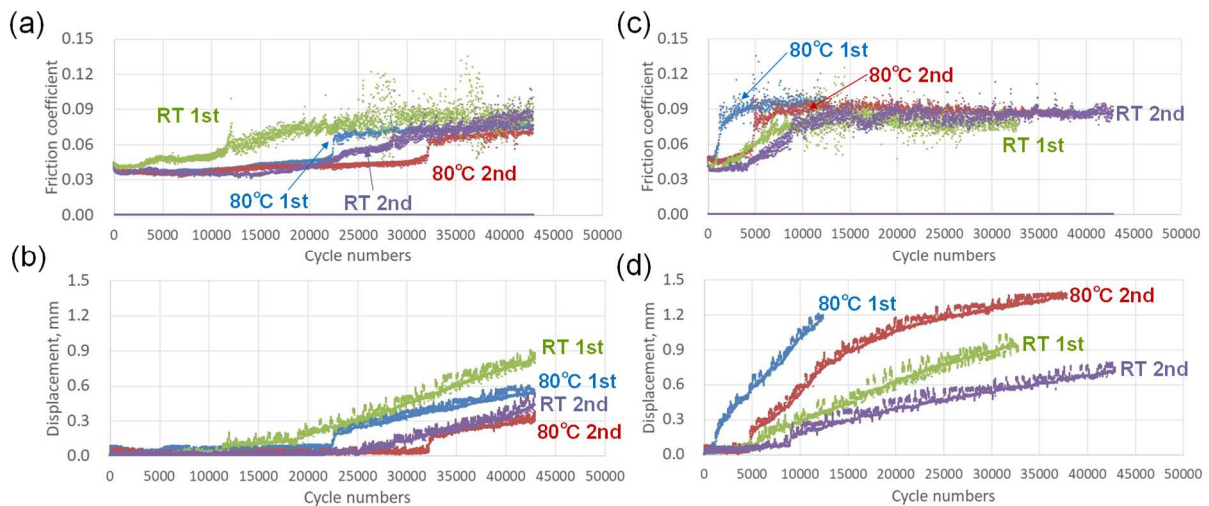


Fig. 15 Evolution of (a) the friction coefficient using the GF composite, (b) the vertical displacement of the GF composite, (c) the friction coefficient using the CF composite, and (d) the vertical displacement of the CF composite at room temperature (RT) and 80 °C under a normal load of 350 N with sliding for 10 s sliding, followed by stopping for 200 s.

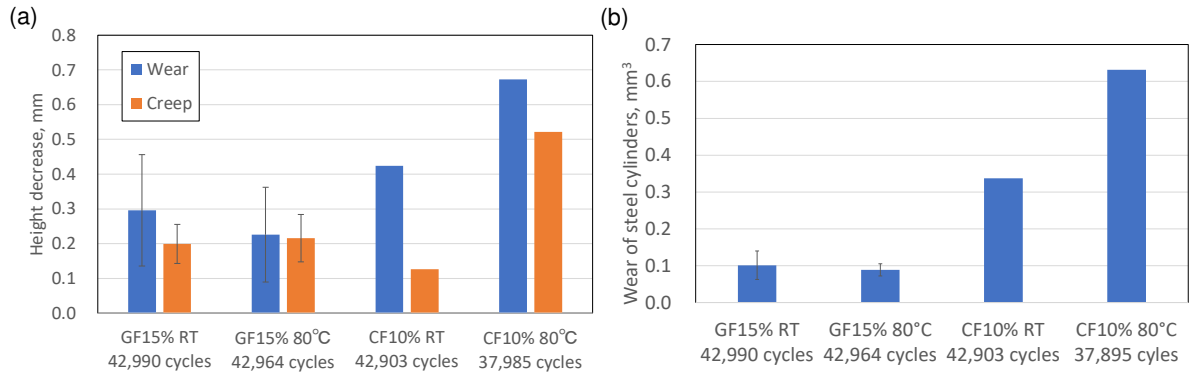


Fig. 16 (a) Wear and creep height loss of the composite and (b) wear of the steel cylinders after the sliding tests under a normal load of 350 N with sliding for 10 s, followed by stopping for 200 s. The values for the GF composite are the average values for 2 different sliding tests.

To discuss the difference in the temperature dependence of the tribological properties between the GF composite and CF composite, tribofilm formation, which is related to the tribochemical reaction of the grease additives, was investigated. The sliding tests that were intentionally stopped before the sudden increases in the friction coefficient and vertical displacement were conducted for the same normal load of 350 N at 80 °C, with sliding for 10 s followed by stopping for 200 s, and the sliding surfaces of the steel cylinders and composite ring were observed and analyzed. The sliding tests using the GF 15 % composite were stopped after 1,018 cycles and 12,595 cycles, and the sliding test using the CF 10 % composite was stopped after 4,752 cycles. Fig. 17 shows the SEM observations of the sliding surfaces of the steel cylinder after ultrasonic washing. For the cylinders tested with the GF composite, randomly distributed dark patches were observed on the sliding surface after both sliding cycles; however, dark patches were rarely visible on the sliding surface of the steel cylinders tested with CF composite. ToF-SIMS (time of flight secondary ion mass spectrometry) analysis of the steel cylinder tested with the GF composite for 12,595 cycles revealed that a tribofilm containing carboxylate (including stearate or palmitate), which is related to the tribochemical reaction of the zinc carboxylate added to the grease, formed on the steel surface [12]. This carboxylate tribofilm had a significant effect on the improvement of the tribological properties at 80 °C and supplemented the degradation of the tribological properties related to the reduced mechanical properties of the GF composite compared to those at room temperature. In addition, the presence of Zn and S was detected on the sliding surface of both the GF composite and CF composite through the SEM-EDX analysis, as shown in Fig. 18. Zn and S were present in the ZnS reactive film, which was detected via X-ray photoelectron spectroscopy (XPS) analysis of the GF composite surface; however, the ZnS reactive film had less effect on the improvement of the tribological properties, as reported in the authors' previous work [12]. Therefore, the difficulty in forming a tribofilm on the steel surface tested with the CF composite can explain why the tribological properties of the CF composite were inferior at 80 °C compared to those at room temperature.

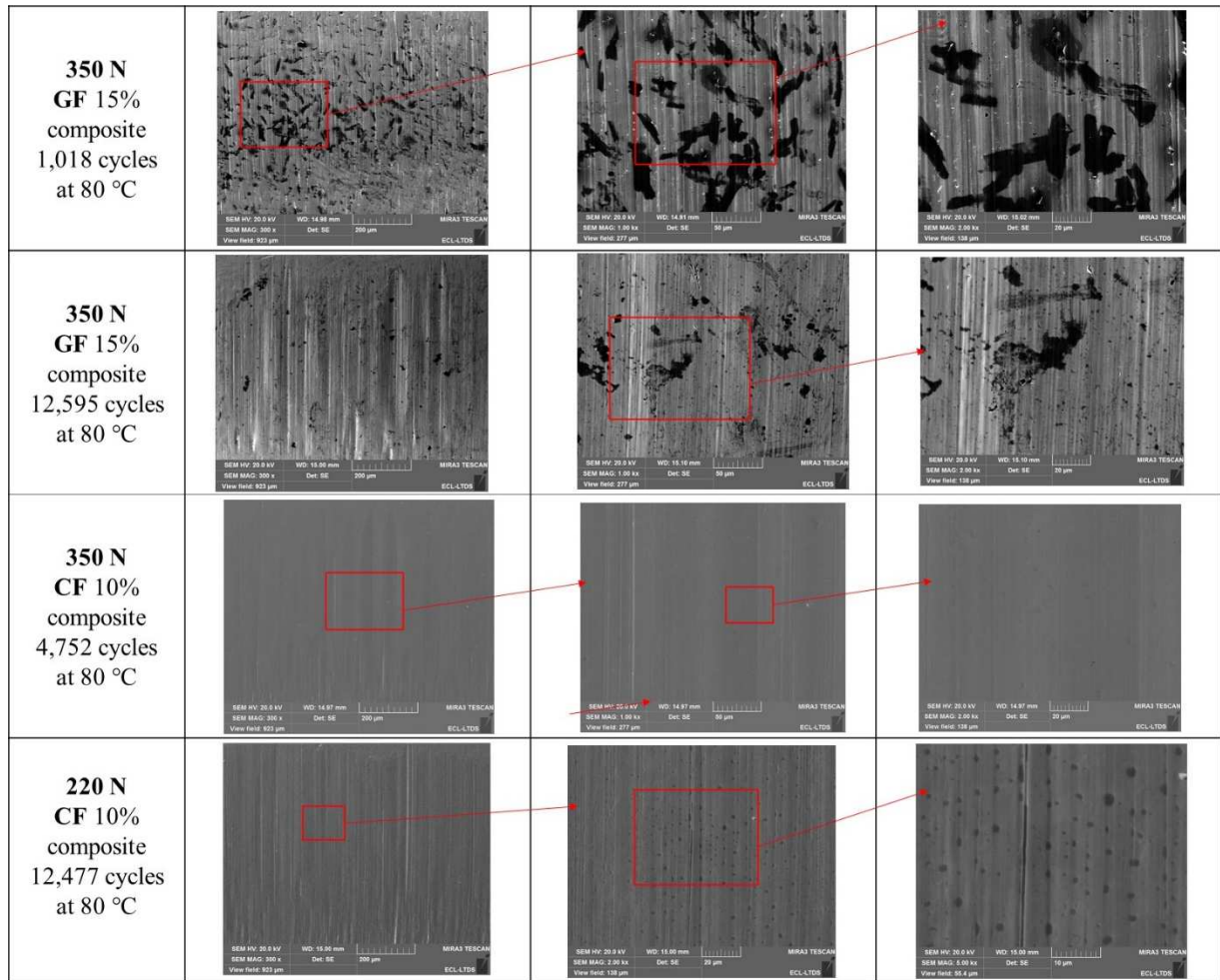


Fig. 17 SEM observations of the sliding surfaces after the sliding tests under different normal loads after different numbers of cycles with sliding for 10 s followed by stopping for 200 s at 80 °C.

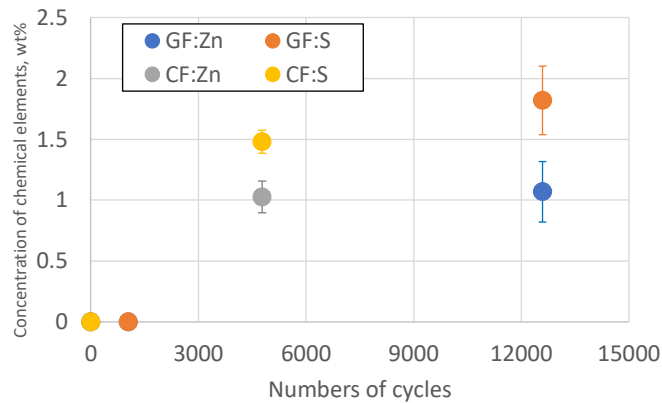


Fig. 18 Concentrations of Zn and S on the composite surface measured via SEM-EDX.

To better understand the difference in the tribochemistry between the CF composite and GF composite, the grease that did not contain zinc carboxylate as a low friction additive (grease no. 2 in Table 3) was prepared and sliding tests were conducted under the same test conditions. Fig. 19 shows the difference in the evolution of the friction coefficient and the vertical displacement using the CF 10 % composite (sample no. 1) and GF 15 %

composite (sample no. 3) under a normal load of 350 N with sliding for 10 s sliding followed by stopping for 200 s at 80 °C. The zinc carboxylate addition to the grease did not significantly influence the tribological properties of the CF composite; only a slight decrease in the friction coefficient was observed. In contrast, the addition of zinc carboxylate significantly improved the tribological properties of the GF composite; a sudden increase in the friction coefficient and vertical displacement was observed after several cycles with the zinc carboxylate, and the displacements (wear and creep of the composite) were lower [12]. These results indicate that zinc carboxylate was not effective at improving the tribological properties when the CF composite was used under this test condition, unlike the GF composite. In addition, these results coincide with the inferior tribological properties exhibited by the CF composite at 80 °C compared to those at room temperature, as presented in Fig. 15, and the formation of the tribofilm on the steel surface was not observed, as shown in Fig. 17.

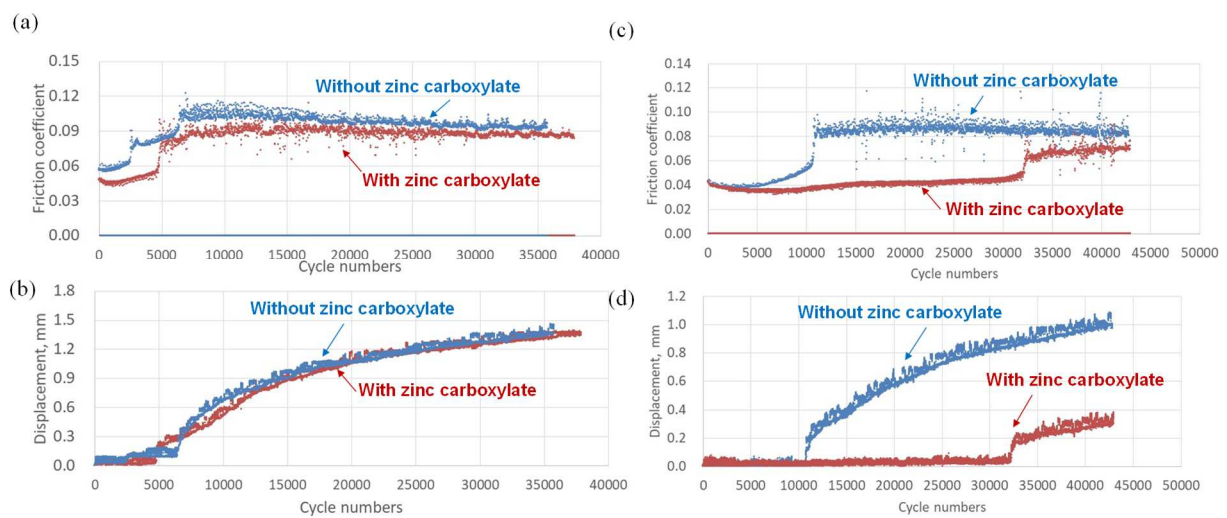


Fig. 19 Evolution of the friction coefficient and vertical displacement using (a, b) the CF 10 % composite and (c, d) the GF 15 % composite and grease, with or without zinc carboxylate in the sliding tests under a normal load of 350 N with sliding for 10 s, sliding followed by stopping for 200 s at 80 °C.

The difference in the formation of the tribofilm on the steel cylinder surface and the effect of the zinc carboxylate under a normal load of 350 N at 80 °C may be attributed to the difference in the contact pressure due to the difference in Young's moduli of the composites or the difference in the tribochemical reaction mechanism related to the fiber type. To clarify the effects of the difference in the contact pressure on the tribochemical reaction mechanism, sliding tests were conducted using the CF composite (sample no. 1) under a normal load of 220 N (at room temperature and 80 °C), with sliding for 10 s followed by stopping for 200 s; the reduced contact pressure was the same as that in the previous sliding test of the GF composite for a normal load of 350 N. Fig. 20 presents the evolution of the friction coefficient, temperature, and vertical displacement from the two sliding tests after 43,044 and 104,114 cycles, respectively. Optical microscope observations of the sliding surfaces after the sliding tests are shown in Fig. S16 in the supplementary material. Unlike the evolutions under a normal load of 350 N (Fig. 15), the vertical displacements (wear and creep) and the rate of the increase in the displacement after the sudden increase were lower at 80 °C than those at room temperature. Fig. 21

presents the wear and creep of the CF composite and wear volume of the steel cylinders (total wear volume of the four cylinders) after the sliding tests during both cycles. The wear height loss of the CF composite was clearly higher at room temperature than that at 80 °C. The wear height loss was higher than the creep height loss at both room temperature and 80 °C, particularly after 104,114 cycles, and no significant difference in the creep height loss was observed between room temperature and 80 °C. The wear volume of the steel cylinders at room temperature was also higher than that at 80 °C. This trend for the wear resistance of the CF composite and steel counterpart was opposite to the results under a normal load of 350 N, as presented in Fig. 16. Therefore, the effect of the contact pressure (normal load) on the tribofilm formation on the steel surface was observed via SEM to elucidate the difference in the tribological properties between the normal loads of 220 N and 350 N.

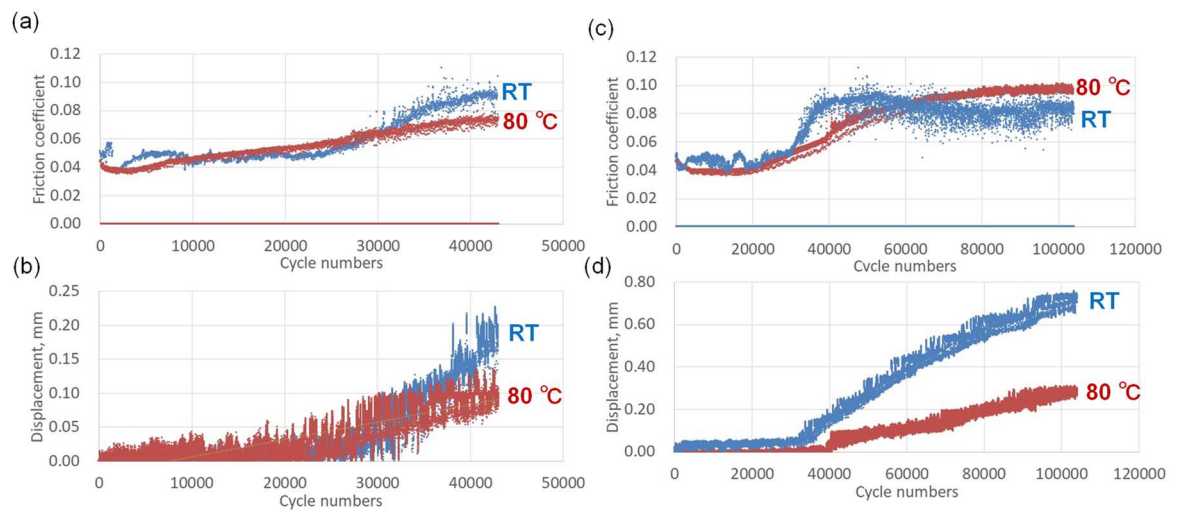


Fig. 20 Evolution of the friction coefficient and vertical displacement using the CF 10% composite and grease with zinc carboxylate in the sliding tests under a normal load of 220 N (at room temperature and 80 °C), with sliding for 10 s followed by stopping for 200 (a, b) over 43,044 cycles and (c, d) over 104,114 cycles.

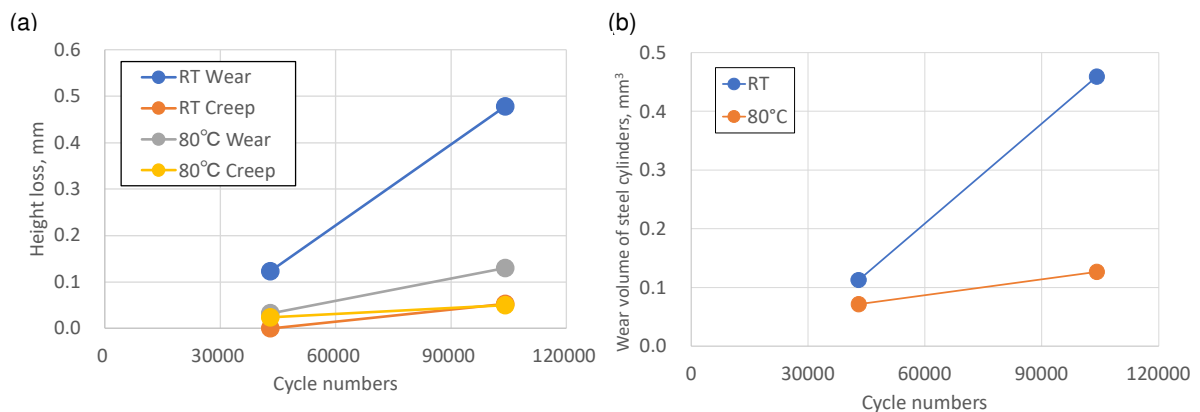


Fig. 21 (a) Wear and creep height loss of the CF composite and (b) wear volume of the steel cylinders after the sliding tests for 43,004 and 104,114 cycles under a normal load of 220 N, with sliding for 10 s followed by stopping for 200 s.

Fig. 17 also presents the SEM observations of the steel cylinder sliding surface after 12,477 cycles (before the sudden increase in the friction coefficient and vertical displacement) under a normal load of 220 N with sliding for 10 s followed by stopping for 200 s at 80 °C. Compared to the observations for a normal load of 350 N (also shown in Fig. 17), a larger number of dark patches were observed on the steel cylinder surface but the surface area of the dark patches on the steel tested with the GF composite under a normal load of 350 N was much larger. These results can explain the difference in the tribological properties of the CF composite at 80 °C between the normal loads of 220 N and 350 N. In the sliding test under 350 N, the contact pressure was too high to form the carboxylate tribofilm on the steel surface (the rate of removal of the tribofilm was much higher than the rate of formation); therefore, the wear of the CF composite increased as the mechanical properties of the composite decreased at high temperature. In contrast, in the sliding test under 220 N, the contact pressure was appropriate for the formation of the tribofilm (the contact pressure was closer to that of the GF 15 % composite under a normal load of 350 N) and the carboxylate tribofilm formation on the steel surface improved the tribological properties, as observed in the GF 15 % composite.

In addition, the effect of the contact pressure on the tribological properties under grease lubrication was investigated for the GF 33 % composite (sample no. 5), which had a higher Young's modulus and generated a higher contact pressure (252 MPa at room temperature) than the GF 15 % composite under the same normal load. Fig. 22 presents the evolution of the friction coefficient and the vertical displacement from the sliding test under a normal load of 350 N, with sliding for 10 s followed by stopping for 200 s, using the GF 33 % composite and grease with/without zinc carboxylate at room temperature and 80 °C. Unlike the GF 15% composite (as presented in Fig. 15 and Fig. 20), the tribological properties at 80 °C were inferior to those at room temperature (a higher vertical displacement at 80 °C than at room temperature) and the addition of zinc carboxylate addition to the grease did not produce any discernable improvements in the tribological properties at 80 °C. These results follow the same trend that was observed for the CF composite under a normal load of 350 N, as presented in Fig. 15. As for the GF 15 % composite, the sliding test was intentionally stopped before the sudden increase in the friction coefficient and vertical displacement; the sliding surfaces on the steel cylinder were observed via SEM to investigate the tribofilm formation relationship with the sliding test results. Fig. 23 presents the SEM observations of the steel surface tested with the GF 33 % composite after 4,745 cycles, lubricated by grease with zinc carboxylate under a normal load of 350 N at 80 °C, with sliding for 10 s followed by stopping for 200 s. Some dark patches, attributed to the carboxylate film, were observed; however, the total area of the patches was markedly lower than that for the cylinders tested with the GF 15 % composite under the same test conditions, as presented in Fig. 17. Therefore, similar to the CF 10 % composite under a normal load of 350 N, the contact pressure was too high to form the tribofilm on the sliding surface of the steel counterpart and the film removal was accelerated. Therefore, the improvement in the tribological properties provided by the carboxylate tribofilm was not obtained and the tribological properties were inferior at 80 °C compared to those at room temperature, exhibiting the same evolution of the displacement (wear and creep of the composite) with and without the zinc carboxylate.

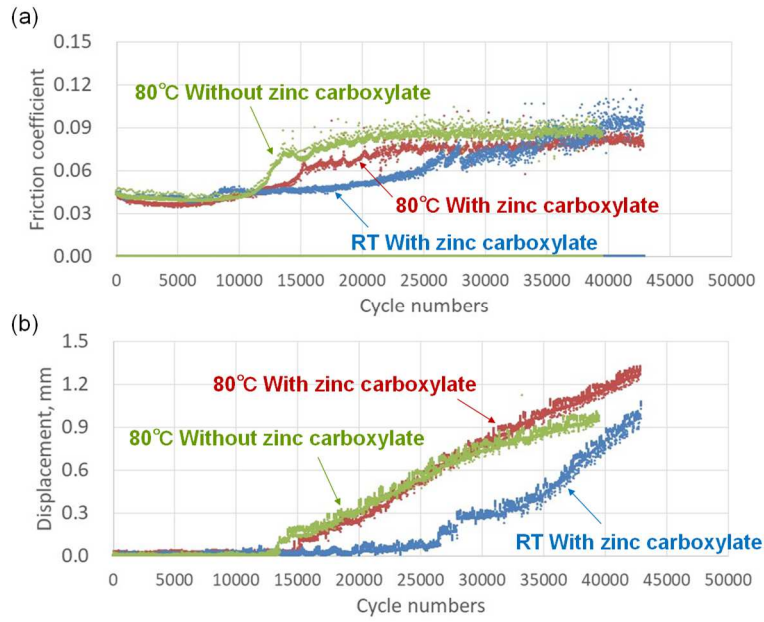


Fig. 22 Evolution of (a) the friction coefficient and (b) the vertical displacement during the sliding tests using the GF 33% composite and grease with/without zinc carboxylate, under a normal load of 350 N (at room temperature and 80 °C), with sliding for 10 s followed by stopping for 200 s.

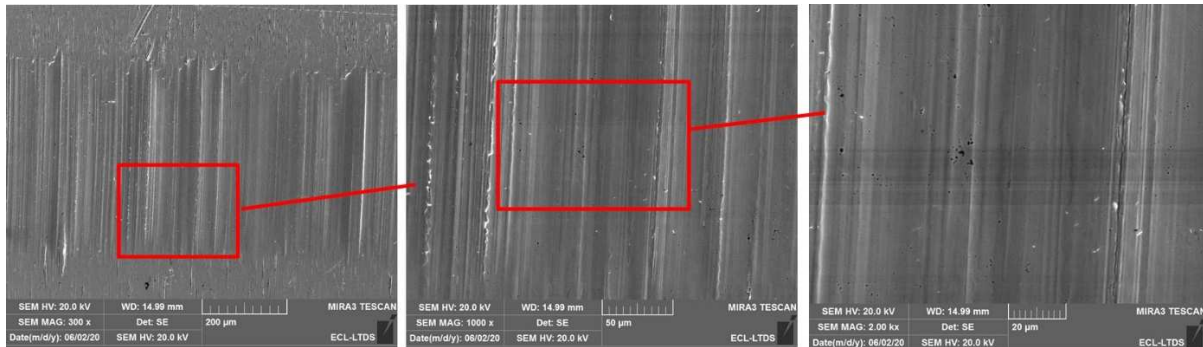


Fig. 23 SEM observations of the steel surface tested with the GF 33% composite after 4,745 cycles under a normal load of 350 N at 80 °C, with sliding for 10 s followed by stopping for 200 s and lubricated by grease with zinc carboxylate.

4. Conclusion

The tribological properties of CF-reinforced PA66 composites in contact with steel under grease lubrication were investigated and compared to those of GF-reinforced PA66. The following conclusions were drawn.

- 1) Under dry conditions, fiber reinforcement led to reduced friction and improved wear resistance compared to unreinforced PA66. The CF composite exhibited lower friction as the adhesive wear resulted in the formation of a low friction transfer film, which was composed of a graphite structure related to the CFs.
- 2) Under grease lubrication, the CF composite presented inferior tribological properties compared to the GF composite, regardless of the molecular mass of PA66 and taking into account the contact pressure difference

related to the difference in Young's moduli. The insufficient interfacial adhesion between the PA66 and CFs induced fiber peeling, which scratched the PA66 at much earlier cycles.

- 3) The destructive effects of the CF composite on the steel counterpart were much higher than those of the GF composite, even though the hardness of the CFs (measured through nanoindentation) was much lower than that of the GFs. The destructive effect is not determined solely by the fiber hardness, and insufficient interfacial adhesion between the CFs and PA66 also led to an increase in the wear of the steel counterpart.
- 4) The difference in the temperature dependence of the tribological properties between the CF composite and GF composite was due to the difference in the tribofilm formation related to the grease additives. The tribofilm formation was dominated by contact pressure, regardless of fiber type, and contributed to the improvement of the tribological properties at 80 °C.

References

- [1] B. Sarita, S. Senthilvelan, Effects of lubricant on the surface durability of an injection molded polyamide 66 spur gear paired with a steel gear, *Tribol. Int.* 137 (2019) 193–211. <https://doi.org/10.1016/j.triboint.2019.02.050>
- [2] S. Kirupasankar, C. Gurunathan. R. Gnanamoorthy, Transmission efficiency of polyamide nanocomposite spur gears, *Mater. Des.* 39 (2012) 338-343. <https://doi.org/10.1016/j.matdes.2012.02.045>
- [3] J. Tavčar, G. Grkman, J. Duhovnik, Accelerated lifetime testing of reinforced polymer gears, *J. Adv. Mec. Des., Sys., and Manuf.* 12 (2018) 1-13. <https://doi.org/10.1299/jamdsm.2018jamdsm0006>
- [4] Y. Zhang, C. Pursell, K. Mao, S. Leigh, A physical investigation of wear and thermal characteristics of 3D printed nylon spur gears. *Tribol. Int.* 141 (2020) 105953. <https://doi.org/10.1016/j.triboint.2019.105953>
- [5] H. Oh, M.H. Azarian, C. Morillo, M. Pecht, E. Rhem, Failure mechanisms of ball bearings under lightly loaded, non-accelerated usage conditions, *Tribol. Int.* 81 (2015) 291–299. <https://doi.org/10.1016/j.triboint.2014.09.014>
- [6] Z. Wenhui, D. Sier, C. Guoding, C. Yongcun, Impact of lubricant traction coefficient on cage's dynamic characteristics in high-speed angular contact ball bearing, *Chin. J. Aeronaut.* 30 (2017) 827-835. <https://doi.org/10.1016/j.cja.2016.08.019>
- [7] M. Harrass, K. Friedrich, A.A. Almajid, Tribological behavior of selected engineering polymers under rolling contact. *Tribol. Int.* 43 (2010) 635–646. <https://doi.org/10.1016/j.triboint.2009.10.003>
- [8] T. Kunishima, K. Miyake, T. Kurokawa, H. Arai, Clarification of tribological behavior on tooth surface of resin worm gear for electric power steering, *JTEKT Eng. J. English Ed.*, 1013E (2016) 27–33.
- [9] S.C. Tung, W.W. Cheng, Simulation test of grease-lubricated steel-polymer interface of worm gear, *Tribol. Trans.* 41 (1998) 537-542. <https://doi.org/10.1080/10402009808983780>
- [10] A. Bormuth, J. Zuleeg, C. Schmitz, R. Schmitz, M. Pfadt and H. Meven, Lubrication of plastic worm gears, *Power Transm. Eng. Aug.* (2019) 42-47.
- [11] T. Kunishima, Y. Nagai, T. Kurokawa, G. Bouvard, J-C. Abry, V. Fridrici, Ph. Kapsa, Tribological behavior of glass fiber reinforced-PA66 in contact with carbon steel under high contact pressure, sliding and grease lubricated conditions, *Wear* 456-457 (2020) 203383. <https://doi.org/10.1016/j.wear.2020.203383>

- [12] T. Kunishima, S. Nagai, T. Kurokawa, J. Galipaud, G. Guillonneau, G. Bouvard, J.-Ch. Abry, C. Minfray, V. Fridrici, Ph. Kapsa, Effects of temperature and addition of zinc carboxylate to grease on the tribological properties of PA66 in contact with carbon steel, *Tribol. Int.* 153 (2021) 106578. <https://doi.org/10.1016/j.triboint.2020.106578>
- [13] T. Kunishima, Y. Nagai, S. Nagai, T. Kurokawa, G. Bouvard, J.-C. Abry, V. Fridrici, P. Kapsa, Effects of glass fiber properties and polymer molecular mass on the mechanical and tribological properties of a polyamide-66-based composite in contact with carbon steel under grease lubrication, *Wear* 462-463 (2020) 203500. <https://doi.org/10.1016/j.wear.2020.203500>
- [14] X. Huang, Fabrication and properties of carbon fibers, *Mater.* 2 (2009) 2369-2403. <https://doi.org/10.3390/ma2042369>
- [15] D.A. Baker, T.G. Rials, Recent advances in low-cost carbon fiber manufacture from lignin, *J. Appl. Polym. Sci.* (2013) 713-728. <https://doi.org/10.1002/app.39273>
- [16] S.V. Joshi, L.T. Drzal, A.K. Mohanty, S. Arorac, Are natural fiber composites environmentally superior to glass fiber reinforced composites?, *Compos. Part A: Appl. Sci. Manuf.* 35 (2004) 371-376. <https://doi.org/10.1016/j.compositesa.2003.09.016>
- [17] U.S. Tewari, J. Bijwe, J.N. Mathur, I. Sharma, Studies on abrasive wear of carbon fibre (short) reinforced polyamide composites, *Tribol. Int.* 25 (1992) 53-60. [https://doi.org/10.1016/0301-679X\(92\)90121-3](https://doi.org/10.1016/0301-679X(92)90121-3)
- [18] S. Zhou, Q. Zhang, C. Wu, J. Huang, Effect of carbon fiber reinforcement on the mechanical and tribological properties of polyamide6/polyphenylene sulfide composites, *Mater. Des.* 44 (2013) 493-499. <https://doi.org/10.1016/j.matdes.2012.08.029>
- [19] S. Senthilvelan, R. Gnanamoorthy, Damage mechanisms in injection molded unreinforced, glass and carbon reinforced nylon 66 spur gears, *Appl. Compos. Mater.* 11 (2004) 377-397. <https://doi.org/10.1023/B:ACMA.0000045313.47841.4e>
- [20] M. Sharma, J. Bijwe, Influence of fiber-matrix adhesion and operating parameters on sliding wear performance of carbon fabric polyethersulphone composites, *Wear* 271 (2011) 2919-2927. <https://doi.org/10.1016/j.wear.2011.06.012>
- [21] J. Li, X.H. Cheng, Friction and wear properties of surface-treated carbon fiber-reinforced thermoplastic polyimide composites under oil-lubricated condition, *Mater. Chem. Phys.* 108 (2008) 67-72. <https://doi.org/10.1016/j.matchemphys.2007.09.003>
- [22] F. Zhao, G. Li, G. Zhang, T. Wang, Q. Wang, Hybrid effect of ZnS sub-micrometer particles and reinforcing fibers on tribological performance of polyimide under oil lubrication conditions, *Wear* 380-381 (2017) 86-95. <https://doi.org/10.1016/j.wear.2017.03.007>
- [23] M. Kurokawa, Y. Uchiyama, S. Nagai, Performance of plastic gear made of carbon fiber reinforced poly-ether-ether-ketone, *Tribol. Int.* 32 (1999) 491-497. [https://doi.org/10.1016/S0301-679X\(99\)00078-X](https://doi.org/10.1016/S0301-679X(99)00078-X)
- [24] G. Wypych, *Handbook of Fillers (Fourth Edition)*, (2016) 252-255. <https://doi.org/10.1016/B978-1-895198-91-1.50004-X>
- [25] J. Theberge, B. Arkles, Wear characteristics of carbon fiber reinforced thermoplastics, *Lubr. Eng.* 30 12 (1974) 585-589.

- [26] J.K. Lancaster, The effect of carbon fibre reinforcement on the friction and wear of polymers, *J. Phys. D: Appl. Phys.* 1 5 (1968) 549-559. <https://doi.org/10.1088/0022-3727/1/5/303>
- [27] T. Kunishima, T. Kurokawa, H. Arai, V. Fridrici, P. Kapsa, Reactive extrusion mechanism, mechanical and tribological behavior of fiber reinforced polyamide 66 with added carbodiimide, *Mater. Des.* 188 (2020) 108447. <https://doi.org/10.1016/j.matdes.2019.108447>
- [28] G. Srinath, R. Gnanamoorthy, Effect of short fibre reinforcement on the friction and wear behaviour of Nylon 66, *Appl. Compos. Mater.* 12 (2005) 369–383. <https://doi.org/10.1007/s10443-005-5824-6>
- [29] B. Suresha, K.S. Kumar, S. Seetharamu, P.S. Kumaran, Friction and dry sliding wear behavior of carbon and glass fabric reinforced vinyl ester composites, *Tribol. Int.* 43 (2010) 602-609. <https://doi.org/10.1016/j.triboint.2009.09.009>
- [30] J. Li, Y.C. Xia, The reinforcement effect of carbon fiber on the friction and wear properties of carbon fiber reinforced PA6 composites, *Fibers Polym.* 10 (2009) 519–525. <https://doi.org/10.1007/s12221-009-0519-5>
- [31] S.N. Kukureka, C.J. Hooke, M. Rao, P. Liao, Y.K. Chen, The effect of fibre reinforcement on the friction and wear of polyamide 66 under dry rolling–sliding contact, *Tribol. Int.* 32 (1999) 107-116. [https://doi.org/10.1016/S0301-679X\(99\)00017-1](https://doi.org/10.1016/S0301-679X(99)00017-1)
- [32] A. Leatherbarrow, H. Wu, Mechanical behaviour of the constituents inside carbon-fibre/carbon-silicon carbide composites characterised by nano-indentation, *J. Eur. Ceram. Soc.* 32 (2012) 579-588. <https://doi.org/10.1016/j.jeurceramsoc.2011.09.026>
- [33] Y. Sun, G. Zhao, F. Yang, Anisotropic behavior of the nanoindentation of single carbon fibers, *Nanosci. Nanotechnol. Lett.* 6 (2014) 596-600. <https://doi.org/10.1166/nnl.2014.1809>